

Search for single-top production in ep collisions at HERA

ZEUS Collaboration

Abstract

A search for single-top production, $ep \rightarrow etX$, has been performed with the ZEUS detector at HERA using data corresponding to an integrated luminosity of 0.37 fb^{-1} . No evidence for top production was found, consistent with the expectation from the Standard Model. Limits were computed for single-top production via flavour changing neutral current transitions involving a neutral electroweak vector boson, γ or Z . The result was combined with a previous ZEUS result yielding a total luminosity of 0.50 fb^{-1} . A 95% credibility level upper limit of 0.13 pb was obtained for the cross section at the centre-of-mass energy of $\sqrt{s} = 315 \text{ GeV}$.

The ZEUS Collaboration

H. Abramowicz^{45,ah}, I. Abt³⁵, L. Adamczyk¹³, M. Adamus⁵⁴, R. Aggarwal^{7,c}, S. Antonelli⁴, P. Antonioli³, A. Antonov³³, M. Arneodo⁵⁰, V. Aushev^{26,27,z}, Y. Aushev^{27,z,aa}, O. Bachynska¹⁵, A. Bamberger¹⁹, A.N. Barakbaev²⁵, G. Barbagli¹⁷, G. Bari³, F. Barreiro³⁰, N. Bartosik^{27,ab}, D. Bartsch⁵, M. Basile⁴, O. Behnke¹⁵, J. Behr¹⁵, U. Behrens¹⁵, L. Bellagamba³, A. Bertolin³⁹, S. Bhadra⁵⁷, M. Bindi⁴, C. Blohm¹⁵, V. Bokhonov^{26,z}, T. Bołd¹³, K. Bondarenko²⁷, E.G. Boos²⁵, K. Borras¹⁵, D. Boscherini³, D. Bot¹⁵, I. Brock⁵, E. Brownson⁵⁶, R. Brugnera⁴⁰, N. Brümmer³⁷, A. Bruni³, G. Bruni³, B. Brzozowska⁵³, P.J. Bussey²⁰, B. Bylsma³⁷, A. Caldwell³⁵, M. Capua⁸, R. Carlin⁴⁰, C.D. Catterall⁵⁷, S. Chekanov¹, J. Chwastowski^{12,e}, J. Ciborowski^{53,al}, R. Ciesielski^{15,g}, L. Cifarelli⁴, F. Cindolo³, A. Contin⁴, A.M. Cooper-Sarkar³⁸, N. Coppola^{15,h}, M. Corradi³, F. Corriveau³¹, M. Costa⁴⁹, G. D'Agostini⁴³, F. Dal Corso³⁹, J. del Peso³⁰, R.K. Dementiev³⁴, S. De Pasquale^{4,a}, M. Derrick¹, R.C.E. Devenish³⁸, D. Dobur^{19,s}, B.A. Dolgoshein^{33,†}, G. Dolinska^{26,27}, A.T. Doyle²⁰, V. Drugakov¹⁶, L.S. Durkin³⁷, S. Dusini³⁹, Y. Eisenberg⁵⁵, P.F. Ermolov^{34,†}, A. Eskreys^{12,†}, S. Fang^{15,i}, S. Fazio⁸, J. Ferrando³⁸, M.I. Ferrero⁴⁹, J. Figiel¹², M. Forrest^{20,v}, B. Foster^{38,ad}, G. Gach¹³, A. Galas¹², E. Gallo¹⁷, A. Garfagnini⁴⁰, A. Geiser¹⁵, I. Gialas^{21,w}, L.K. Gladilin^{34,ac}, D. Gladkov³³, C. Glasman³⁰, O. Gogota^{26,27}, Yu.A. Golubkov³⁴, P. Göttlicher^{15,j}, I. Grabowska-Bołd¹³, J. Grebenyuk¹⁵, I. Gregor¹⁵, G. Grigorescu³⁶, G. Grzelak⁵³, O. Gueta⁴⁵, M. Guzik¹³, C. Gwenlan^{38,ae}, T. Haas¹⁵, W. Hain¹⁵, R. Hamatsu⁴⁸, J.C. Hart⁴⁴, H. Hartmann⁵, G. Hartner⁵⁷, E. Hilger⁵, D. Hochman⁵⁵, R. Hori⁴⁷, K. Horton^{38,af}, A. Hüttmann¹⁵, Z.A. Ibrahim¹⁰, Y. Iga⁴², R. Ingbir⁴⁵, M. Ishitsuka⁴⁶, H.-P. Jakob⁵, F. Januschek¹⁵, T.W. Jones⁵², M. Jünger⁵, I. Kadenko²⁷, B. Kahle¹⁵, S. Kananov⁴⁵, T. Kanno⁴⁶, U. Karshon⁵⁵, F. Karstens^{19,t}, I.I. Katkov^{15,k}, M. Kaur⁷, P. Kaur^{7,c}, A. Keramidis³⁶, L.A. Khein³⁴, J.Y. Kim⁹, D. Kisieleska¹³, S. Kitamura^{48,aj}, R. Klanner²², U. Klein^{15,l}, E. Koffeman³⁶, P. Kooijman³⁶, Ie. Korol^{26,27}, I.A. Korzhavina^{34,ac}, A. Kotański^{14,f}, U. Kötz¹⁵, H. Kowalski¹⁵, O. Kuprash¹⁵, M. Kuze⁴⁶, A. Lee³⁷, B.B. Levchenko³⁴, A. Levy⁴⁵, V. Libov¹⁵, S. Limentani⁴⁰, T.Y. Ling³⁷, M. Lisovyi¹⁵, E. Lobodzinska¹⁵, W. Lohmann¹⁶, B. Lühr¹⁵, E. Lohrmann²², K.R. Long²³, A. Longhin³⁹, D. Lontkovskiy¹⁵, O.Yu. Lukina³⁴, J. Maeda^{46,ai}, S. Magill¹, I. Makarenko¹⁵, J. Malka¹⁵, R. Mankel¹⁵, A. Margotti³, G. Marini⁴³, J.F. Martin⁵¹, A. Mastroberardino⁸, M.C.K. Mattingly², I.-A. Melzer-Pellmann¹⁵, S. Mergelmeyer⁵, S. Miglioranzi^{15,m}, F. Mohamad Idris¹⁰, V. Monaco⁴⁹, A. Montanari¹⁵, J.D. Morris^{6,b}, K. Mujkic^{15,n}, B. Musgrave¹, K. Nagano²⁴, T. Namsou^{15,o}, R. Nania³, A. Nigro⁴³, Y. Ning¹¹, T. Nobe⁴⁶, U. Noor⁵⁷, D. Notz¹⁵, R.J. Nowak⁵³, A.E. Nuncio-Quiroz⁵, B.Y. Oh⁴¹, N. Okazaki⁴⁷, K. Oliver³⁸, K. Olkiewicz¹², Yu. Onishchuk²⁷, K. Papageorgiu²¹, A. Parenti¹⁵, E. Paul⁵, J.M. Pawlak⁵³, B. Pawlik¹², P. G. Pelfer¹⁸, A. Pellegrino³⁶, W. Perlański^{53,am}, H. Perrey¹⁵, K. Piotrkowski²⁹, P. Pluciński^{54,an}, N.S. Pokrovskiy²⁵, A. Polini³, A.S. Proskuryakov³⁴, M. Przybycień¹³, A. Raval¹⁵, D.D. Reeder⁵⁶, B. Reisert³⁵, Z. Ren¹¹, J. Repond¹, Y.D. Ri^{48,ak}, A. Robertson³⁸, P. Roloff^{15,m}, I. Rubinsky¹⁵, M. Ruspa⁵⁰, R. Sacchi⁴⁹, A. Saliı̄²⁷, U. Samson⁵, G. Sartorelli⁴, A.A. Savin⁵⁶, D.H. Saxon²⁰, M. Schioppa⁸, S. Schlenstedt¹⁶, P. Schleper²², W.B. Schmidke³⁵, U. Schneekloth¹⁵, V. Schönberg⁵, T. Schörner-Sadenius¹⁵, J. Schwartz³¹, F. Sciulli¹¹, L.M. Shcheglova³⁴, R. Shehzadi⁵, S. Shimizu^{47,m}, I. Singh^{7,c}, I.O. Skillicorn²⁰, W. Słomiński¹⁴, W.H. Smith⁵⁶, V. Sola⁴⁹, A. Solano⁴⁹, D. Son²⁸, V. Sosnovtsev³³, A. Spiridonov^{15,p}, H. Stadie²², L. Stanco³⁹, A. Stern⁴⁵, T.P. Stewart⁵¹, A. Stifutkin³³, P. Stopa¹², S. Suchkov³³, G. Susinno⁸, L. Suszycki¹³, J. Sztuk-Dambietz²², D. Szuba²², J. Szuba^{15,q}, A.D. Tapper²³, E. Tassi^{8,d}, J. Terrón³⁰, T. Theedt¹⁵, H. Tiecke³⁶, K. Tokushuku^{24,x}, O. Tomalak²⁷, J. Tomaszewska^{15,r},

T. Tsurugai³², M. Turcato²², T. Tymieniecka^{54,ao}, M. Vázquez^{36,m}, A. Verbytskyi¹⁵, O. Viazlo^{26,27}, N.N. Vlasov^{19,u}, O. Volynets²⁷, R. Walczak³⁸, W.A.T. Wan Abdullah¹⁰, J.J. Whitmore^{41,ag}, L. Wiggers³⁶, M. Wing⁵², M. Wlasenko⁵, G. Wolf¹⁵, H. Wolfe⁵⁶, K. Wrona¹⁵, A.G. Yagües-Molina¹⁵, S. Yamada²⁴, Y. Yamazaki^{24,y}, R. Yoshida¹, C. Youngman¹⁵, A.F. Żarnecki⁵³, L. Zawiejski¹², O. Zenaiev¹⁵, W. Zeuner^{15,m}, B.O. Zhautykov²⁵, N. Zhmak^{26,z}, C. Zhou³¹, A. Zichichi⁴, Z. Zolkapli¹⁰, M. Zolko²⁷, D.S. Zotkin³⁴

1 *Argonne National Laboratory, Argonne, Illinois 60439-4815, USA*^A
 2 *Andrews University, Berrien Springs, Michigan 49104-0380, USA*
 3 *INFN Bologna, Bologna, Italy*^B
 4 *University and INFN Bologna, Bologna, Italy*^B
 5 *Physikalisches Institut der Universität Bonn, Bonn, Germany*^C
 6 *H.H. Wills Physics Laboratory, University of Bristol, Bristol, United Kingdom*^D
 7 *Panjab University, Department of Physics, Chandigarh, India*
 8 *Calabria University, Physics Department and INFN, Cosenza, Italy*^B
 9 *Institute for Universe and Elementary Particles, Chonnam National University,*
Kwangju, South Korea
 10 *Jabatan Fizik, Universiti Malaya, 50603 Kuala Lumpur, Malaysia*^E
 11 *Nevis Laboratories, Columbia University, Irvington on Hudson, New York 10027,*
USA^F
 12 *The Henryk Niewodniczanski Institute of Nuclear Physics, Polish Academy of*
Sciences, Krakow, Poland^G
 13 *AGH-University of Science and Technology, Faculty of Physics and Applied Com-*
puter Science, Krakow, Poland^H
 14 *Department of Physics, Jagellonian University, Cracow, Poland*
 15 *Deutsches Elektronen-Synchrotron DESY, Hamburg, Germany*
 16 *Deutsches Elektronen-Synchrotron DESY, Zeuthen, Germany*
 17 *INFN Florence, Florence, Italy*^B
 18 *University and INFN Florence, Florence, Italy*^B
 19 *Fakultät für Physik der Universität Freiburg i.Br., Freiburg i.Br., Germany*
 20 *School of Physics and Astronomy, University of Glasgow, Glasgow, United King-*
dom^D
 21 *Department of Engineering in Management and Finance, Univ. of the Aegean, Chios,*
Greece
 22 *Hamburg University, Institute of Experimental Physics, Hamburg, Germany*^I
 23 *Imperial College London, High Energy Nuclear Physics Group, London, United King-*
dom^D
 24 *Institute of Particle and Nuclear Studies, KEK, Tsukuba, Japan*^J
 25 *Institute of Physics and Technology of Ministry of Education and Science of Kaza-*
khstan, Almaty, Kazakhstan
 26 *Institute for Nuclear Research, National Academy of Sciences, Kyiv, Ukraine*
 27 *Department of Nuclear Physics, National Taras Shevchenko University of Kyiv, Kyiv,*
Ukraine
 28 *Kyungpook National University, Center for High Energy Physics, Daegu, South*
Korea^K
 29 *Institut de Physique Nucléaire, Université Catholique de Louvain, Louvain-la-Neuve,*
Belgium^L
 30 *Departamento de Física Teórica, Universidad Autónoma de Madrid, Madrid,*
Spain^M
 31 *Department of Physics, McGill University, Montréal, Québec, Canada H3A 2T8*^N
 32 *Meiji Gakuin University, Faculty of General Education, Yokohama, Japan*^J
 33 *Moscow Engineering Physics Institute, Moscow, Russia*^O
 34 *Moscow State University, Institute of Nuclear Physics, Moscow, Russia*^P
 35 *Max-Planck-Institut für Physik, München, Germany*
 36 *NIKHEF and University of Amsterdam, Amsterdam, Netherlands*^Q
 37 *Physics Department, Ohio State University, Columbus, Ohio 43210, USA*^A
 38 *Department of Physics, University of Oxford, Oxford, United Kingdom*^D

39 *INFN Padova, Padova, Italy*^B
40 *Dipartimento di Fisica dell' Università and INFN, Padova, Italy*^B
41 *Department of Physics, Pennsylvania State University, University Park,*
Pennsylvania 16802, USA^F
42 *Polytechnic University, Sagamihara, Japan*^J
43 *Dipartimento di Fisica, Università 'La Sapienza' and INFN, Rome, Italy*^B
44 *Rutherford Appleton Laboratory, Chilton, Didcot, Oxon, United Kingdom*^D
45 *Raymond and Beverly Sackler Faculty of Exact Sciences, School of Physics,*
Tel Aviv University, Tel Aviv, Israel^R
46 *Department of Physics, Tokyo Institute of Technology, Tokyo, Japan*^J
47 *Department of Physics, University of Tokyo, Tokyo, Japan*^J
48 *Tokyo Metropolitan University, Department of Physics, Tokyo, Japan*^J
49 *Università di Torino and INFN, Torino, Italy*^B
50 *Università del Piemonte Orientale, Novara, and INFN, Torino, Italy*^B
51 *Department of Physics, University of Toronto, Toronto, Ontario, Canada M5S*
1A7^N
52 *Physics and Astronomy Department, University College London, London, United*
Kingdom^D
53 *Faculty of Physics, University of Warsaw, Warsaw, Poland*
54 *National Centre for Nuclear Research, Warsaw, Poland*
55 *Department of Particle Physics and Astrophysics, Weizmann Institute, Rehovot, Is-*
rael
56 *Department of Physics, University of Wisconsin, Madison, Wisconsin 53706, USA*^A
57 *Department of Physics, York University, Ontario, Canada M3J 1P3*^N

- A* supported by the US Department of Energy
- B* supported by the Italian National Institute for Nuclear Physics (INFN)
- C* supported by the German Federal Ministry for Education and Research (BMBF), under contract No. 05 H09PDF
- D* supported by the Science and Technology Facilities Council, UK
- E* supported by an FRGS grant from the Malaysian government
- F* supported by the US National Science Foundation. Any opinion, findings and conclusions or recommendations expressed in this material are those of the authors and do not necessarily reflect the views of the National Science Foundation.
- G* supported by the Polish Ministry of Science and Higher Education as a scientific project No. DPN/N188/DESY/2009
- H* supported by the Polish Ministry of Science and Higher Education and its grants for Scientific Research
- I* supported by the German Federal Ministry for Education and Research (BMBF), under contract No. 05h09GUF, and the SFB 676 of the Deutsche Forschungsgemeinschaft (DFG)
- J* supported by the Japanese Ministry of Education, Culture, Sports, Science and Technology (MEXT) and its grants for Scientific Research
- K* supported by the Korean Ministry of Education and Korea Science and Engineering Foundation
- L* supported by FNRS and its associated funds (IISN and FRIA) and by an Inter-University Attraction Poles Programme subsidised by the Belgian Federal Science Policy Office
- M* supported by the Spanish Ministry of Education and Science through funds provided by CICYT
- N* supported by the Natural Sciences and Engineering Research Council of Canada (NSERC)
- O* partially supported by the German Federal Ministry for Education and Research (BMBF)
- P* supported by RF Presidential grant N 4142.2010.2 for Leading Scientific Schools, by the Russian Ministry of Education and Science through its grant for Scientific Research on High Energy Physics and under contract No.02.740.11.0244
- Q* supported by the Netherlands Foundation for Research on Matter (FOM)
- R* supported by the Israel Science Foundation

- a* now at University of Salerno, Italy
- b* now at Queen Mary University of London, United Kingdom
- c* also funded by Max Planck Institute for Physics, Munich, Germany
- d* also Senior Alexander von Humboldt Research Fellow at Hamburg University, Institute of Experimental Physics, Hamburg, Germany
- e* also at Cracow University of Technology, Faculty of Physics, Mathematics and Applied Computer Science, Poland
- f* supported by the research grant No. 1 P03B 04529 (2005-2008)
- g* now at Rockefeller University, New York, NY 10065, USA
- h* now at DESY group FS-CFEL-1
- i* now at Institute of High Energy Physics, Beijing, China
- j* now at DESY group FEB, Hamburg, Germany
- k* also at Moscow State University, Russia
- l* now at University of Liverpool, United Kingdom
- m* now at CERN, Geneva, Switzerland
- n* also affiliated with Universtiy College London, UK
- o* now at Goldman Sachs, London, UK
- p* also at Institute of Theoretical and Experimental Physics, Moscow, Russia
- q* also at FPACS, AGH-UST, Cracow, Poland
- r* partially supported by Warsaw University, Poland
- s* now at Istituto Nucleare di Fisica Nazionale (INFN), Pisa, Italy
- t* now at Haase Energie Technik AG, Neumünster, Germany
- u* now at Department of Physics, University of Bonn, Germany
- v* now at Biodiversität und Klimaforschungszentrum (BiK-F), Frankfurt, Germany
- w* also affiliated with DESY, Germany
- x* also at University of Tokyo, Japan
- y* now at Kobe University, Japan
- z* supported by DESY, Germany
- † deceased
- aa* member of National Technical University of Ukraine, Kyiv Polytechnic Institute, Kyiv, Ukraine
- ab* member of National University of Kyiv - Mohyla Academy, Kyiv, Ukraine
- ac* partly supported by the Russian Foundation for Basic Research, grant 11-02-91345-DFG_a
- ad* Alexander von Humboldt Professor; also at DESY and University of Oxford
- ae* STFC Advanced Fellow
- af* nee Korcsak-Gorzo
- ag* This material was based on work supported by the National Science Foundation, while working at the Foundation.
- ah* also at Max Planck Institute for Physics, Munich, Germany, External Scientific Member
- ai* now at Tokyo Metropolitan University, Japan
- aj* now at Nihon Institute of Medical Science, Japan
- ak* now at Osaka University, Osaka, Japan
- al* also at Łódź University, Poland
- am* member of Łódź University, Poland
- an* now at Department of Physics, Stockholm University, Stockholm, Sweden

^{oo} also at Cardinal Stefan Wyszyński University, Warsaw, Poland

1 Introduction

The dominant production process of single top quarks in the Standard Model (SM) in ep collisions¹ at HERA is the charged current (CC) reaction $ep \rightarrow \nu t X$ [1], which has a cross section of less than 1 fb [2]. Flavour changing neutral current (FCNC) processes could enhance single-top production, but they are strongly suppressed in the SM by the GIM mechanism [3]. This mechanism forbids FCNCs at the tree level, allowing only for small contributions at the one-loop level, exploiting the flavour mixing due to the CKM matrix [4]. Several extensions of the SM predict FCNC contributions already at the tree level [5]. The search for such new interactions involving the top quark (ut or ct transitions mediated by neutral vector bosons, γ or Z) opens an interesting window to look for effects beyond the SM [6].

The FCNC couplings tuV and tcV , with $V = \gamma, Z$, have been investigated in $p\bar{p}$ collisions at the Tevatron, where searches for the top-quark decays $t \rightarrow uV$ and $t \rightarrow cV$ [7,8] were carried out. The Tevatron experiments also constrained the couplings tug and tcg [9] which induce FCNC transitions mediated by the gluon. The couplings tuV and tcV were also investigated in e^+e^- interactions at LEP2 by searching for single-top production through the reactions $e^+e^- \rightarrow t\bar{u} (+c.c.)$ and $e^+e^- \rightarrow t\bar{c} (+c.c.)$ [10, 11]. No evidence for such interactions was found and limits were set on the branching ratios $\text{Br}(t \rightarrow q\gamma)$ and $\text{Br}(t \rightarrow qZ)$, with $q = u, c$.

The same FCNC couplings could induce single-top production in ep collisions, $ep \rightarrow etX$ [12], in which the incoming lepton exchanges a γ or Z with an up quark in the proton, yielding a top quark in the final state, see Fig. 1. Owing to the large Z mass, this process is more sensitive to a coupling of the type $tq\gamma$. Furthermore, large values of x , the fraction of the proton momentum carried by the struck quark, are needed to produce a top quark. Since the u -quark parton distribution function (PDF) of the proton is dominant at large x , the production of single top quark is most sensitive to the $tu\gamma$ coupling.

In the present study, the top signal was searched for by looking for the decays $t \rightarrow bev_e$ and $t \rightarrow b\mu\nu_\mu$. At HERA, such event topologies with one lepton with high transverse momentum, p_T , and large missing transverse momentum originate predominantly from single- W production, which has a cross section of about 1 pb [13] and is the most important background to any top signal. The present analysis extends the previously published ZEUS results [14] which used data from the HERA I running period², corresponding to a total integrated luminosity of 0.13 fb^{-1} . The integrated luminosity used in this analysis is about three times larger. A combination of the results from the two running periods (total integrated luminosity 0.50 fb^{-1}) has been performed.

¹Here and in the following, e denotes both the electron and the positron.

²Data collected between 1994 and 2000.

2 Theoretical framework

The effects of the FCNC transitions induced by couplings of the type tuV are parameterised using the following effective Lagrangian [15]:

$$\Delta\mathcal{L}_{\text{eff}} = e e_t \bar{t} \frac{i\sigma_{\mu\nu} p^\nu}{\Lambda} \kappa_\gamma u A^\mu + \frac{g}{2 \cos \theta_W} \bar{t} \gamma_\mu v_Z u Z^\mu + \text{h.c.} \quad (1)$$

where κ_γ and v_Z are two FCNC couplings mediating ut transitions, e (e_t) is the electron (top quark) electric charge, g is the weak coupling constant, θ_W is the weak mixing angle, $\sigma_{\mu\nu} = \frac{1}{2}(\gamma^\mu\gamma^\nu - \gamma^\nu\gamma^\mu)$, Λ is an effective cut-off parameter which, by convention, is set to the mass of the t quark, M_t , p is the momentum of the gauge boson and A^μ (Z^μ) is the photon (Z) field. In the following, it is assumed that the magnetic coupling κ_γ and the vector coupling v_Z are real and positive.

The cross section for the process $ep \rightarrow etX$ was evaluated at the leading order (LO) using the package CompHEP-4.5.1 [16] and was parameterised in terms of three parameters describing the effects of the two FCNC couplings, A_σ and B_σ , and their interference, C_σ :

$$\sigma_{ep \rightarrow etX} = A_\sigma \kappa_\gamma^2 + B_\sigma v_Z^2 + C_\sigma \kappa_\gamma v_Z. \quad (2)$$

The decay widths of the top in the different channels were also evaluated using CompHEP-4.5.1:

$$\Gamma_{t \rightarrow u\gamma} = A_\Gamma \kappa_\gamma^2, \quad \Gamma_{t \rightarrow uZ} = B_\Gamma v_Z^2, \quad \Gamma_{t \rightarrow qW} = C_\Gamma, \quad (3)$$

where A_Γ and B_Γ are the partial width of the top corresponding to $u\gamma$ and uZ unitary FCNC couplings, respectively, and C_Γ is the SM top width.

The above parameters, summarised in Table 1, were evaluated using the top mass $M_t = 172.0 \pm 1.6$ GeV [17] and the PDF set CTEQ6L1 [18]. The interference parameter C_σ has only a small effect, producing a cross section variation of less than 0.5% in the whole range of the couplings considered in this analysis, and was therefore neglected. The QCD corrections to the LO cross-section were evaluated at the approximate next-to-leading order (NLO) and next-to-next-to-leading order (NNLO) [12, 19] for magnetic couplings both at the γ and Z vertices. Since we considered a different coupling (vector coupling) at the Z vertex, we used such corrections only to evaluate the limits for the γ exchange (see Sect. 7.1). Such corrections increase the LO cross-section by 15% and slightly reduces the uncertainties due to the QCD factorisation-scale (see Sect. 6). The limits involving both coupling (see Sect. 7.2) were evaluated using the LO cross-section.

3 Experimental setup

The analysis is based on ep collisions recorded with the ZEUS detector during the HERA II running period³, using an integrated luminosity of 0.37 fb^{-1} , divided into two approximately

³Data collected between 2004 and 2007.

equal samples of e^+p and e^-p collisions. The lepton beams were polarised, with roughly equal luminosities for positive and negative polarisation, such that the average polarisation was negligible for this analysis.

A detailed description of the ZEUS detector can be found elsewhere [20]. A brief outline of the components that are most relevant for this analysis is given below.

Charged particles were tracked in the central tracking detector (CTD) [21] which operated in a magnetic field of 1.43 T provided by a thin superconducting solenoid. The CTD consisted of 72 cylindrical drift chamber layers, organised in nine superlayers covering the polar-angle⁴ region $15^\circ < \theta < 164^\circ$. The CTD was complemented by a silicon microvertex detector (MVD) [22], consisting of three active layers in the barrel and four disks in the forward region. For CTD-MVD tracks that pass through all nine CTD superlayers, the momentum resolution was $\sigma(p_T)/p_T = 0.0029p_T \oplus 0.0081 \oplus 0.0012/p_T$ with p_T in GeV.

The high-resolution uranium–scintillator calorimeter (CAL) [23] consisted of three parts: the forward (FCAL), the barrel (BCAL) and the rear (RCAL) calorimeters. Each part was subdivided transversely into towers and longitudinally into one electromagnetic section (EMC) and either one (in RCAL) or two (in BCAL and FCAL) hadronic sections (HAC). The smallest subdivision of the calorimeter was called a cell. The CAL energy resolutions, as measured under test-beam conditions, were $\sigma(E)/E = 0.18/\sqrt{E}$ for electrons and $\sigma(E)/E = 0.35/\sqrt{E}$ for hadrons, with E in GeV.

The luminosity was measured using the Bethe-Heitler reaction $ep \rightarrow e\gamma p$ by a luminosity detector which consisted of a lead–scintillator calorimeter [24] and an independent magnetic spectrometer [25]. The fractional uncertainty on the measured luminosity was 1.9%.

4 Monte Carlo simulation

Samples of events were generated using Monte Carlo (MC) simulations to determine the selection efficiency for single-top events produced through FCNC processes and to estimate background rates from SM processes. The generated events were passed through the GEANT-3.21 [26] ZEUS detector- and trigger-simulation programs [20]. They were reconstructed and analysed by the same program chain as the data.

Single-top samples were generated with COMPHEP 4.5.1, interfaced with PYTHIA 6.14 [27] for parton showering, hadronisation and particle decay. The mass of the top quark in COMPHEP was set to $M_t = 175$ GeV. Different sets were produced for the two different production processes (γ - and Z -mediated) and for the two decay modes ($t \rightarrow bW$ and $t \rightarrow uZ$).

Alternative sets were also generated, only for the γ -mediated process, with the HEXF generator [28] assuming top-quark masses of 170 and 175 GeV. These sets were used to study

⁴The ZEUS coordinate system is a right-handed Cartesian system, with the Z axis pointing in the proton beam direction, referred to as the “forward direction”, and the X axis pointing towards the centre of HERA. The coordinate origin is at the nominal interaction point. The pseudorapidity is defined as $\eta = -\ln(\tan \frac{\theta}{2})$, where the polar angle, θ , is measured with respect to the proton beam direction.

the small effect of M_t variation, in order to correct the selection efficiency, evaluated using the COMPHEP samples, for the different M_t values used in the generation and in the cross-section calculation (see Sect. 2). Initial-state radiation from the lepton beam was included using the Weizsäcker-Williams approximation [29]. The hadronic final state was simulated using the matrix-element and parton-shower model of LEPTO [30] for the QCD cascade and the Lund string model [31] as implemented in JETSET [32] for the hadronisation. The results for COMPHEP and the alternative samples agree within uncertainties.

Standard Model single- W production is the most significant background to top production. Another important background in the electron-decay channel of the W ($t \rightarrow bW \rightarrow be\nu$) arises from neutral current (NC) deep inelastic scattering (DIS). In addition, two-photon processes provide a source of high- p_T leptons that are a significant background in the muon-decay channel of the W ($t \rightarrow bW \rightarrow b\mu\nu$). The CC DIS is a minor source of background for both channels.

The following MC programs were used to simulate the different background processes. Single- W production was simulated using the event generator EPVEC [33] which did not include hard QCD radiation. The $ep \rightarrow eWX$ and $ep \rightarrow \nu WX$ events from EPVEC were scaled by a factor dependent on the transverse momentum and rapidity of the W , such that the resulting cross section corresponded to a calculation including QCD corrections at next-to-leading order [34].

Neutral current and CC DIS events were simulated using the LEPTO 6.5 program [30], interfaced to HERACLES 4.6.1 [35] via DJANGO 1.1 [36]. The HERACLES program includes photon and Z exchanges and first-order electroweak radiative corrections. The QCD cascade was modelled with the colour-dipole model [37] by using the ARIADNE 4.08 program [38].

Two-photon processes were simulated using the generator GRAPE 1.1 [39], which includes dilepton production via $\gamma\gamma$, $Z\gamma$ and ZZ processes and considers both elastic and inelastic production at the proton vertex.

5 Event selection

The event selection was optimised for single-top production via photon exchange, looking for the dominant decay $t \rightarrow bW$ and subsequent W decay to e and μ and their respective neutrinos. The selection is based on requiring an isolated high- p_T lepton and a large missing transverse momentum.

Cosmic background, relevant especially for the muon channel, was suppressed using timing cuts based on calorimeter measurements and the track impact parameter with respect to the beam spot. Further cosmic background overlapping with ep interactions was rejected by applying a cut $E - p_z < 60$ GeV, $E - p_z$ being the sum of the total and longitudinal energy deposits of the cells in the calorimeter. For fully contained events, $E - p_z$ is twice the electron-beam energy and peaks at 55 GeV.

Events from beam-gas interactions were rejected on the basis of the ratio of the number of tracks pointing to the vertex to the total number of tracks in an event.

5.1 Online selection

A three-level trigger system was used to select events online [40]. At the first level, coarse calorimeter and tracking information were available. Events were selected using criteria based on either the transverse energy or missing transverse momentum measured in the CAL. Events were accepted with a low threshold on these quantities when a coincidence with CTD tracks from the event vertex was found, while a higher threshold was used for events with no CTD tracks.

At the second level, timing information from the CAL was used to reject events inconsistent with an ep interaction. In addition, the topology of the CAL energy deposits was used to reject non- ep background events. In particular, a tighter cut was made on missing transverse momentum, since the resolution in this variable was better at the second than at the first level.

At the third level, track reconstruction and vertex finding were performed and used to reject events with a vertex inconsistent with ep interactions. Cuts were applied to calorimeter quantities and reconstructed tracks to further reduce beam-gas contamination.

5.2 Offline selection

Jets, used in the selection to define lepton isolation, were reconstructed from CAL cells using the k_T cluster algorithm [41] in the longitudinally invariant inclusive mode [42] and were corrected for energy loss due to the dead material in front of the CAL. The jets were required to have a transverse energy $E_T^{\text{jet}} > 4.5 \text{ GeV}$ and pseudorapidity $|\eta^{\text{jet}}| < 2.5$.

Muon selection

Muons were reconstructed by matching calorimeter cell-patterns compatible with a minimum-ionising particle to CTD tracks [43]. Events were selected as follows:

- $|Z_{\text{vtx}}| < 30 \text{ cm}$, Z_{vtx} being the Z coordinate of the interaction vertex, to restrict to a region compatible with ep interactions;
- $E - p_Z > 10 \text{ GeV}$. The $E - p_Z$ of the CAL deposit associated with the muon was replaced by that of the muon track. This requirement rejected photoproduction events, which populate the low $E - p_Z$ region;
- $P_T^{\text{miss}} > 10 \text{ GeV}$, P_T^{miss} being the missing transverse momentum measured by the CAL;
- at least one muon candidate with the following characteristics:
 - a track from the primary vertex matched with a CTD track with at least three hit superlayers and a transverse momentum, p_T^μ , greater than 8 GeV ;

- the distance, ΔR , of the muon candidate in the pseudorapidity-azimuth (η - ϕ) plane with respect to any other track and jet in the event satisfying $\Delta R = \sqrt{(\Delta\eta)^2 + (\Delta\phi)^2} > 0.5$.

A total of 269 events were selected, while 260 ± 3 (stat.) were expected from the SM, which is dominated by the dimuon production from the $\gamma\gamma$ process. The quoted uncertainty is the error on the expected SM prediction due to the MC statistics.

Figure 2 shows the comparison between data and MC for the variables p_T^μ , θ^μ , acoplanarity (ϕ^{acop}), P_T^{miss} , transverse mass (M_T), hadronic transverse momentum (P_T^{had}). Here P_T^{had} , M_T and ϕ^{acop} are defined as follows:

- $P_T^{\text{had}} = \sqrt{(\sum_i P_X^i)^2 + (\sum_i P_Y^i)^2}$, where P_X^i and P_Y^i are the X and Y components of the CAL energy deposits not associated with the lepton;
- $M_T = \sqrt{2p_T^l p_T^{\nu} (1 - \cos \phi^{l\nu})}$, where p_T^l is the lepton transverse momentum, p_T^{ν} is the modulus of the missing P_T vector obtained from the CAL and corrected using track information to account for muons, $\phi^{l\nu}$ is the azimuthal separation between the lepton and the missing P_T vector;
- ϕ^{acop} is the angle between the lepton and the vector balancing the P_T^{had} and is defined for events with P_T^{had} greater than 1 GeV.

Reasonable agreement is observed in all cases.

Electron selection

Electrons were reconstructed using an algorithm that combined information from the cluster of the energy deposits in the calorimeter with tracks [44]. Events were selected as follows:

- $|Z_{\text{ vtx}}| < 30$ cm;
- $5 < E - p_Z < 50$ GeV, to reject NC DIS and photoproduction background;
- $P_T^{\text{miss}} > 12$ GeV;
- at least one electron candidate with the following characteristics:
 - $p_T^{\text{el}} > 10$ GeV;
 - $0.3 < \theta^{\text{el}} < 2$ rad;
 - isolated from other tracks and jets in the event, $\Delta R > 0.5$;
 - the extrapolation of the track associated with the electron into the CAL should have a distance of closest approach to the CAL cluster centre < 10 cm and a reconstructed momentum $p > 5$ GeV;
- $M_T > 10$ GeV, to reject events with P_T^{miss} along the electron direction;
- $0.1 < \phi^{\text{acop}} < (\pi - 0.1)$ rad, to reject badly reconstructed NC DIS events with P_T^{miss} in the direction of the electron or of the jet.

A total of 245 events were selected, while 253 ± 6 (stat.) were expected from the SM, which is dominated by the NC DIS process. The quoted uncertainty is the error on the expected SM prediction due to the MC statistics.

Figure 3 shows the comparison between data and MC for the variables p_T^{el} , θ^{el} , ϕ^{acop} , P_T^{miss} , M_T , P_T^{had} . Reasonable agreement is observed in all cases.

5.3 Selection of single-top candidates

Since no excess of events above the SM expectation was observed, a further selection was made to maximise the sensitivity to a possible FCNC single top signal. A cut on P_T^{had} of 40 GeV was applied to both decay channels while the cuts on ϕ^{acop} and P_T^{miss} were optimised separately for the two channels:

- $P_T^{\text{had}} > 40$ GeV for both channels;

muon channel:

- $\phi^{\text{acop}} > 0.05$ rad;
- events with more than one isolated muon were rejected;

electron channel:

- $\phi^{\text{acop}} > 0.15$ rad;
- $P_T^{\text{miss}} > 15$ GeV.

One event survived the selection cuts in the electron channel while three events were found in the muon channel. Table 2 summarises the results of the final selection. In order to compare the MC to data, the P_T^{had} cut was relaxed to 25 GeV. Figures 4 (a) and (b) show the P_T^{had} behaviour for data and SM expectations for the muon and electron channels, respectively. Good agreement between data and predictions is observed for both channels. Also shown are the expectations for top production through FCNC, normalised to the limit on the signal cross section obtained in Sect. 7.1. The data do not support a significant contribution from this process.

6 Systematic uncertainties

The following systematic uncertainties were taken into account:

- the theoretical uncertainty on the W background normalisation was assumed to be $\pm 15\%$ [34];
- the statistical uncertainty on the total SM prediction after the final selection was $\pm 13\%$ and $\pm 9\%$ for the e - and μ -channel, respectively;

- the uncertainty on the NC DIS background, particularly relevant for the e -channel, was evaluated using a sample of events enriched in NC DIS by replacing the $E - p_Z$ and acoplanarity cuts by $E - p_Z > 40$ GeV and $\phi^{\text{acop}} < 0.3$. A systematic uncertainty of $\pm 15\%$ on this source was determined by the level of agreement between data and MC for such a selection. The effect of this uncertainty on the final selection SM prediction was $\pm 6\%$ for the e -channel and negligible for the μ -channel;
- the uncertainty on the electromagnetic and the hadronic CAL energy scale was assumed to be $\pm 1\%$ and $\pm 2\%$, respectively. The two scale uncertainties, summed in quadrature, produced a variation of $\pm 6\%$ and of $\pm 5\%$ on the final SM predictions for the e - and the μ -channel, respectively, while the effect on the signal selection efficiencies was below 2% and was therefore neglected;
- the uncertainty on the top mass, 172.0 ± 1.6 GeV [17], produced a variation on the parameters of the signal cross section and decay widths as reported in Table 1 and a variation of $\pm 2\%$ on the signal selection efficiencies;
- the uncertainties on the signal efficiency due to the statistics of the MC samples are reported in Table 3 for the different channels and decay processes;
- the uncertainties on the PDFs gave a variation on the parameters of the signal cross section as reported in Table 1. Such uncertainties were evaluated as suggested by the CTEQ group [18];
- the uncertainty due to the QCD factorisation-scale affected the signal cross section by $\pm 9\%$ for the LO calculation and by ${}^{+8\%}_{-7\%}$ including the approximated NLO and NNLO QCD corrections (see Sect. 2). This effect was evaluated by varying the central value, set to M_t , between $M_t/2$ and $2M_t$;
- the uncertainty on the luminosity determination was $\pm 1.9\%$.

The uncertainties due to the W normalisation, CAL energy scale, top mass, PDFs and luminosity were assumed to be correlated for the different channels and datasets. All the above uncertainties were included in the limit calculation as explained in Sect. 7.1.

7 Limits on FCNC

Since no excess over the SM prediction was observed, limits on FCNC couplings of the type tuV were evaluated using the results of Table 2. As a first step, limits were evaluated on the signal cross section and on the κ_γ coupling assuming $v_Z = 0$. In a second step, the effect of a non-zero v_Z coupling was accounted for. Limits on the anomalous top branching ratios, $\text{Br}(t \rightarrow u\gamma)$ ($\text{Br}_{u\gamma}$) and $\text{Br}(t \rightarrow uZ)$ (Br_{uZ}), were evaluated.

7.1 Limits on the cross section and κ_γ

The limit on the anomalous top-production cross section was evaluated using a Bayesian approach and assuming a constant prior in the cross section, σ :

$$f(\sigma|\text{data}) = \frac{\prod_i P(N_i^{\text{obs}}|\sigma) f_0(\sigma)}{\int_0^\infty \prod_i P(N_i^{\text{obs}}|\sigma) f_0(\sigma) d\sigma}, \quad (4)$$

$$P(N_i^{\text{obs}}|\sigma) = \frac{\mu_i^{N_i^{\text{obs}}} e^{-\mu_i}}{N_i^{\text{obs}}!}, \quad (5)$$

$$\begin{aligned} \mu_i &= N_i^{\text{sig}} + N_i^{\text{bg}}, \\ N_i^{\text{sig}} &= \sigma \mathcal{L}_i \epsilon_i, \end{aligned}$$

where $f(\sigma|\text{data})$ is the posterior probability density function (p.d.f.) of the signal cross section, $f_0(\sigma)$ its prior, i runs over the different channels and datasets, N_i^{obs} is the number of events surviving the event selection, N_i^{sig} and N_i^{bg} are the number of signal events and the expected SM background, \mathcal{L}_i is the integrated luminosity and ϵ_i the signal efficiency including branching ratio for each decay channel (see the first row in Table 3). The branching ratio of the top to $u\gamma$ was taken into account in the limits evaluation, the selection efficiency for such channel is expected to be low and was therefore set to zero. The systematic uncertainties were treated as nuisance parameters (NPs) and included in the limit calculation, integrating out their dependence (marginalisation) assuming Gaussian priors⁵. The marginalisation over the NPs and the extraction of the posterior p.d.f. was performed using the package *Bayesian Analysis Toolkit* [45], which carries out multidimensional integration using the Markov Chain Monte Carlo technique.

The 95% Credibility Level (C.L.) limit on the cross section was evaluated by integrating the posterior p.d.f.

$$\int_0^{\sigma_{95}} f(\sigma|\text{data}) d\sigma = 0.95, \quad (6)$$

and found to be

$$\sigma < 0.24 \text{ pb (95\% C.L.) at } \sqrt{s} = 318 \text{ GeV}. \quad (7)$$

The limit on the cross section was converted into a limit on the coupling κ_γ , assuming a vanishing v_Z coupling and using the A_σ parameter described in Sect. 2 taking into account the approximated NLO and NNLO QCD corrections (see Sect. 2):

$$\kappa_\gamma < 0.17 \text{ (95\% C.L.)}. \quad (8)$$

The limit is similar to that obtained by ZEUS from HERA I data [46] with an integrated luminosity of 0.13 fb^{-1} . In the HERA I data, no events were found in either the electron

⁵In case of unphysical values, the Gaussian priors were truncated.

or muon channel and also the hadronic W -decay channel was exploited.

The present result was combined with the HERA I limit for a total integrated luminosity of 0.50 fb^{-1} , using the same Bayesian approach as described above and assuming full correlation for the systematic uncertainties due to the W normalisation, CAL energy scale, top mass and PDFs.

The combined cross-section and κ_γ limits are:

$$\sigma < 0.13 \text{ pb (95\% C.L.) at } \sqrt{s} = 315 \text{ GeV,} \quad (9)$$

$$\kappa_\gamma < 0.12 \text{ (95\% C.L.).} \quad (10)$$

The combined cross-section limit corresponds to a centre-of-mass energy of 315 GeV since part of the HERA I data was collected at $\sqrt{s} = 300 \text{ GeV}$.

7.2 Limits on the top anomalous branching ratios

Following the Bayesian approach described above, a two-dimensional posterior p.d.f.,

$$f(\text{Br}_{u\gamma}, \text{Br}_{uZ} | \text{data}), \quad (11)$$

was evaluated combining the HERA I and HERA II datasets. Such a p.d.f. was built using the parameters described in Sect. 2 (no higher-order QCD corrections were applied in this case) to express the FCNC cross-section in terms of the anomalous top branching ratios. The signal efficiencies for the different production channels (γ - or Z -mediated) and decay modes (bW or uZ) were taken into account (see Table 3). The selection efficiency of the e -channel is larger for the Z -mediated process than the γ -mediated process, since in this case the final-state electron is scattered at a larger angle and is more often visible in the detector.

The decay channel $t \rightarrow u\gamma$ was not simulated since the branching ratio is very low for the range of couplings under consideration. In addition, the selection efficiency is expected to be low for such events and was therefore set to zero.

The 95% C.L. boundary in the $(\text{Br}_{u\gamma}, \text{Br}_{uZ})$ plane was evaluated as the set of points

$$f(\text{Br}_{u\gamma}, \text{Br}_{uZ} | \text{data}) = \rho_0,$$

where ρ_0 was chosen such that

$$\int \int_{f(\text{Br}_{u\gamma}, \text{Br}_{uZ} | \text{data}) > \rho_0} d\text{Br}_{u\gamma} d\text{Br}_{uZ} f(\text{Br}_{u\gamma}, \text{Br}_{uZ} | \text{data}) = 0.95. \quad (12)$$

Figure 5 shows the ZEUS boundary in the $(\text{Br}_{u\gamma}, \text{Br}_{uZ})$ plane compared to limits from H1 [47] and from experiments at other colliders: ALEPH [10] at LEP (other LEP experiments [11] have similar results), CDF [7] and D0 [8] at Tevatron. The e^+e^- and hadron colliders, contrary to HERA, have similar sensitivity to u - and c -quark; their limits are hence on both decays $t \rightarrow qV$ with $q = u, c$. The limits set by the ZEUS experiment in the region where Br_{uZ} is less than 4% are the best to date.

8 Conclusions

A search for possible deviations from the Standard Model predictions due to flavour-changing neutral current top production in events with high- p_T leptons and high missing transverse momentum was performed using an integrated luminosity of 0.37 fb^{-1} , collected by the ZEUS detector in 2004–2007. Since no significant deviation from the expectation was observed, the results were used to put limits on the anomalous production of single top quarks at HERA.

A 95% credibility-level upper limit on the cross section of $\sigma < 0.24 \text{ pb}$ at a centre-of-mass energy of 318 GeV was obtained. The limit was combined with a previous ZEUS result, obtained using HERA I data, for a total integrated luminosity of 0.50 fb^{-1} , giving a combined 95% credibility-level upper limit of $\sigma < 0.13 \text{ pb}$ at $\sqrt{s} = 315 \text{ GeV}$. This limit, assuming a vanishing coupling of the top quark to the Z boson, v_Z , corresponds to a constraint on the coupling of the top to the γ , κ_γ , of $\kappa_\gamma < 0.12$. Constraints on the anomalous top branching ratios $t \rightarrow u\gamma$ and $t \rightarrow uZ$ were also evaluated assuming a non-zero v_Z . For low values of v_Z , resulting in branching ratios of $t \rightarrow uZ$ of less than 4%, this paper provides the current best limits.

Acknowledgements

We appreciate the contributions to the construction and maintenance of the ZEUS detector of many people who are not listed as authors. The HERA machine group and the DESY computing staff are especially acknowledged for their success in providing excellent operation of the collider and the data-analysis environment. We thank the DESY directorate for their strong support and encouragement.

References

- [1] G.A. Schuler, Nucl. Phys. B 299 (1988) 21;
U. Baur and J.J. van der Bij, Nucl. Phys. B 304 (1988) 451;
J.J. van der Bij and G.J. van Oldenborgh, Z. Phys. C 51 (1991) 477.
- [2] T. Stelzer, Z. Sullivan and S. Willenbrock, Phys. Rev. D 56 (1997) 5919;
S. Moretti and K. Odagiri, Phys. Rev. D 57 (1998) 3040.
- [3] S.L. Glashow, J. Iliopoulos and L. Maiani, Phys. Rev. D 2 (1970) 1285.
- [4] B. Grzadkowski, J.F. Gunion and P. Krawczyk, Phys. Lett. B 268 (1991) 106;
G. Eilam, J.L. Hewett and A. Soni, Phys. Rev. D 44 (1991) 1473;
M.E. Luke and M.J. Savage, Phys. Lett. B 307 (1993) 387.
- [5] D. Atwood, L. Reina and A. Soni, Phys. Rev. D 53 (1996) 1199;
G.M. de Divitiis, R. Petronzio and L. Silvestrini, Nucl. Phys. B 504 (1997) 45;
R.D. Peccei and X. Zhang, Nucl. Phys. B 337 (1990) 269;
H. Fritzsch and D. Holtmannspötter, Phys. Lett. B 457 (1999) 186.
- [6] H. Fritzsch, Phys. Lett. B 224 (1989) 423;
T. Han, R.D. Peccei and X. Zhang, Nucl. Phys. B 454 (1995) 527.
- [7] CDF Collaboration, F. Abe et al., Phys. Rev. Lett. 80 (1998) 2525.
- [8] D0 Collaboration, V.M. Abazov et al., Phys. Lett. B 701 (2011) 313.
- [9] CDF Collaboration, T. Aaltonen et al., Phys. Rev. Lett. 102 (2009) 151801;
D0 Collaboration, V.M. Abazov et al., Phys. Lett. B 693 (2010) 81.
- [10] ALEPH Collaboration, A. Heister et al., Phys. Lett. B 543 (2002) 173.
- [11] OPAL Collaboration, G. Abbiendi et al., Phys. Lett. B 521 (2001) 181;
L3 Collaboration, P. Achard et al., Phys. Lett. B 549 (2002) 290;
DELPHI Collaboration, J. Abdallah et al., Phys. Lett. B 590 (2004) 21.
- [12] A. Belyaev and N. Kidonakis, Phys. Rev. D 65 (2002) 037501.
- [13] ZEUS Collaboration, S. Chekanov et al., Phys. Lett. B 672 (2009) 106 ;
H1 Collaboration, F.D. Aaron et al., Eur. Phys. J. C 64 (2009) 251;
H1 and ZEUS Collaborations, F.D. Aaron et al., JHEP 1003 (2010) 035.
- [14] ZEUS Collaboration, S. Chekanov et al., Phys. Lett. B 559 (2003) 153.
- [15] T. Han and J.L. Hewett, Phys. Rev. D 60 (1999) 074015.
- [16] E. Boos et al., Nucl. Inst. Meth. A 534 (2004) 250;
A. Pukhov et al., *CompHEP - a package for evaluation of Feynman diagrams and integration over multi-particle phase space. User's manual for version 3.3, INP MSU report 98-41/542.*
- [17] K. Nakamura et al. (Particle Data Group), J. Phys. G 37 (2010) 075021.

- [18] J. Pumplin et al., JHEP 0207 (2002) 012.
- [19] A. Belyaev and N. Kidonakis, JHEP 0312 (2003) 004.
- [20] ZEUS Collaboration, U. Holm (ed.), *The ZEUS Detector*. Status Report (unpublished), DESY (1993), available on <http://www-zeus.desy.de/bluebook/bluebook.html>.
- [21] N. Harnew et al., Nucl. Inst. Meth. A 279 (1989) 290;
B. Foster et al., Nucl. Phys. Proc. Suppl. B 32 (1993) 181;
B. Foster et al., Nucl. Inst. Meth. A 338 (1994) 254.
- [22] A. Polini et al., Nucl. Inst. Meth. A 581 (2007) 656.
- [23] M. Derrick et al., Nucl. Inst. Meth. A 309 (1991) 77;
A. Andresen et al., Nucl. Inst. Meth. A 309 (1991) 101;
A. Caldwell et al., Nucl. Inst. Meth. A 321 (1992) 356;
A. Bernstein et al., Nucl. Inst. Meth. A 336 (1993) 23.
- [24] J. Andrusków et al., Preprint DESY-92-066, DESY, 1992;
ZEUS Collaboration, M. Derrick et al., Z. Phys. C 63 (1994) 391;
J. Andrusków et al., Acta Phys. Pol. B 32 (2001) 2025.
- [25] M. Helbich et al., Nucl. Inst. Meth. A 565 (2006) 572.
- [26] R. Brun et al., GEANT3, Technical Report CERN-DD/EE/84-1, CERN, 1987.
- [27] T. Sjöstrand et al., Comp. Phys. Comm. 135 (2001) 238.
- [28] H.J. Kim and S. Kartik, Preprint LSUHE-145-1993, 1993.
- [29] Ch. Berger and W. Wagner, Phys. Rep. 146 (1987) 1.
- [30] G. Ingelman, A. Edin and J. Rathsman, Comp. Phys. Comm. 101 (1997) 108.
- [31] B. Andersson et al., Phys. Rep. 97 (1983) 31.
- [32] T. Sjöstrand, Comp. Phys. Comm. 39 (1986) 347;
T. Sjöstrand and M. Bengtsson, Comp. Phys. Comm. 43 (1987) 367.
- [33] U. Baur, J.A.M. Vermaseren and D. Zeppenfeld, Nucl. Phys. B 375 (1992) 3.
- [34] K.-P.O. Diener, C. Schwanenberger and M. Spira, Eur. Phys. J. C 25 (2002) 405;
P. Nason, R. Rückl and M. Spira, J. Phys. G 25 (1999) 1434.
- [35] A. Kwiatkowski, H. Spiesberger and H.-J. Möhring, Comp. Phys. Comm. 69 (1992) 155. Also in *Proc. Workshop Physics at HERA*, eds. W. Buchmüller and G. Ingelman, (DESY, Hamburg, 1991);
H. Spiesberger, *An Event Generator for ep Interactions at HERA Including Radiative Processes (Version 4.6)*, 1996, available on <http://www.desy.de/~hspiesb/heracles.html>.
- [36] K. Charchula, G.A. Schuler and H. Spiesberger, Comp. Phys. Comm. 81 (1994) 381;
H. Spiesberger, HERACLES and DJANGO: *Event Generation for ep Interactions at*

HERA Including Radiative Processes, 1998, available on
<http://www.desy.de/~hspiesb/djangoh.html>.

- [37] Y.I. Azimov et al., Phys. Lett. B 165 (1985) 147;
G. Gustafson, Phys. Lett. B 175 (1986) 453;
G. Gustafson and U. Pettersson, Nucl. Phys. B 306 (1988) 746;
B. Andersson et al., Z. Phys. C 43 (1989) 625.
- [38] L. Lönnblad, Comp. Phys. Comm. 71 (1992) 15.
- [39] T. Abe, Comp. Phys. Comm. 136 (2001) 126.
- [40] W.H. Smith, K. Tokushuku and L.W. Wiggers, *Proc. Computing in High-Energy Physics (CHEP), Annecy, France, Sept. 1992*, C. Verkerk and W. Wojcik (eds.), p. 222. CERN, Geneva, Switzerland (1992). Also in preprint DESY 92-150B; P.D. Allfrey et al., Nucl. Inst. Meth. A 580 (2007) 1257.
- [41] S. Catani et al., Nucl. Phys. B 406 (1993) 187.
- [42] S.D. Ellis and D.E. Soper, Phys. Rev. D 48 (1993) 3160.
- [43] V.A. Kuzmin, Nucl. Inst. Meth. A 453 (2000) 336.
- [44] ZEUS Collaboration, J. Breitweg et al., Eur. Phys. J. C 11 (1999) 427.
- [45] A. Caldwell, D. Kollar and K. Kröniger, Comp. Phys. Comm. 180 (2009) 2197.
- [46] ZEUS Collaboration, S. Chekanov et al., Phys. Lett. B 559 (2003) 153.
- [47] H1 Collaboration, F.D. Aaron et al., Phys. Lett. B 678 (2009) 450.

parameter	value	M_t syst.	PDF syst.
A_σ	7.71 pb	$\mp 7\%$	$\pm 4\%$
B_σ	0.296 pb	$\mp 7\%$	$\pm 6\%$
C_σ	-0.016 pb	-	-
A_Γ	0.299 GeV	$\pm 1\%$	-
B_Γ	1.36 GeV	$\pm 4\%$	-
C_Γ	1.48 GeV	$\pm 3\%$	-

Table 1: Parameters used to evaluate single-top production cross sections and decay widths for the different channels. The systematic effects due to the uncertainties on the top mass and the parton distribution functions are also reported.

	N^{obs}	N^{pred}	$W[\%]$
electron channel e^+p	0	1.7 ± 0.4	53 ± 11
muon channel e^+p	1	1.5 ± 0.2	64 ± 9
electron channel e^-p	1	1.9 ± 0.4	51 ± 11
muon channel e^-p	2	1.5 ± 0.3	63 ± 9
electron channel ep	1	3.6 ± 0.6	52 ± 9
muon channel ep	3	3.0 ± 0.4	64 ± 7

Table 2: Number of events passing the final selection cuts, N^{obs} , compared to the SM prediction, N^{pred} . The last column shows the W contribution as a percentage of the total SM expectation. The uncertainties have been obtained by adding systematic and statistical contributions in quadrature.

coupling	decay	e -channel		μ -channel	
		ϵ	$\Delta\epsilon/\epsilon$	ϵ	$\Delta\epsilon/\epsilon$
κ_γ	$t \rightarrow bW$	0.029	± 0.04	0.029	± 0.04
κ_γ	$t \rightarrow uZ$	0.0080	± 0.08	0.011	± 0.07
v_Z	$t \rightarrow bW$	0.048	± 0.04	0.024	± 0.06
v_Z	$t \rightarrow uZ$	0.066	± 0.03	0.012	± 0.07

Table 3: Summary of selection efficiencies on signal samples for different production couplings and decay modes. The relative errors are due to the statistics of the MC samples.

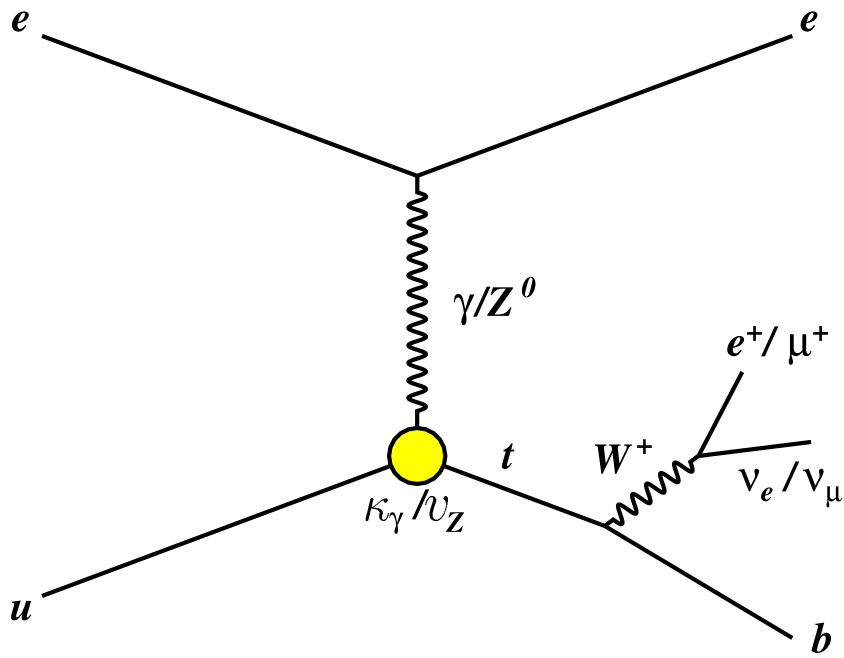


Figure 1: Anomalous single-top production via flavour changing neutral current transitions at HERA with subsequent decays $t \rightarrow bW^+$ and $W^+ \rightarrow \nu_e(\nu_\mu)e^+(\mu^+)$.

ZEUS

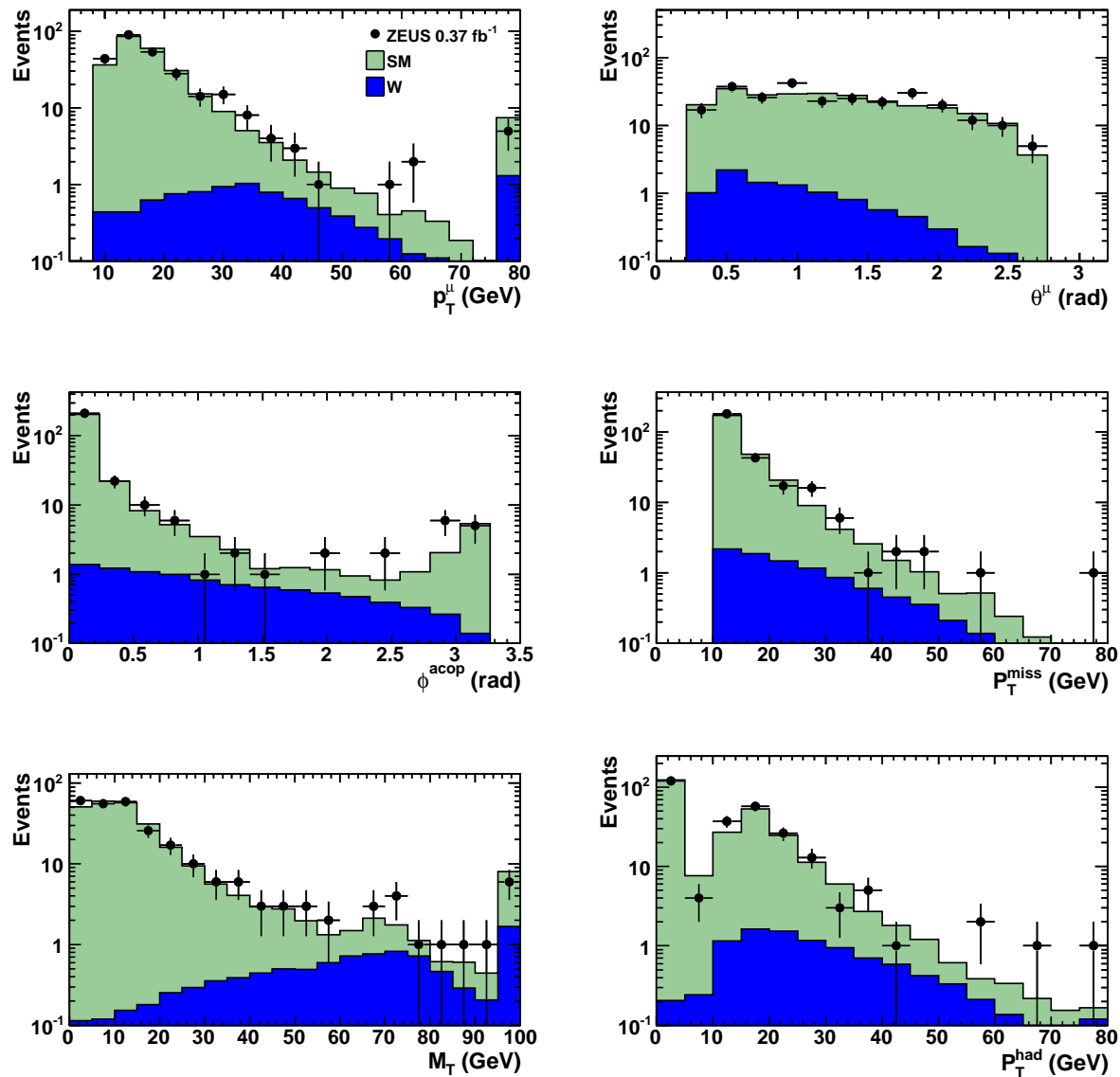


Figure 2: Comparison between data and SM expectations for several variables in the muon channel: p_T^μ , θ^μ , ϕ^{acop} , P_T^{miss} , M_T , P_T^{had} . The contribution of single-W production is also shown as the dark-shaded region. Any histogram overflows are included in the last bin.

ZEUS

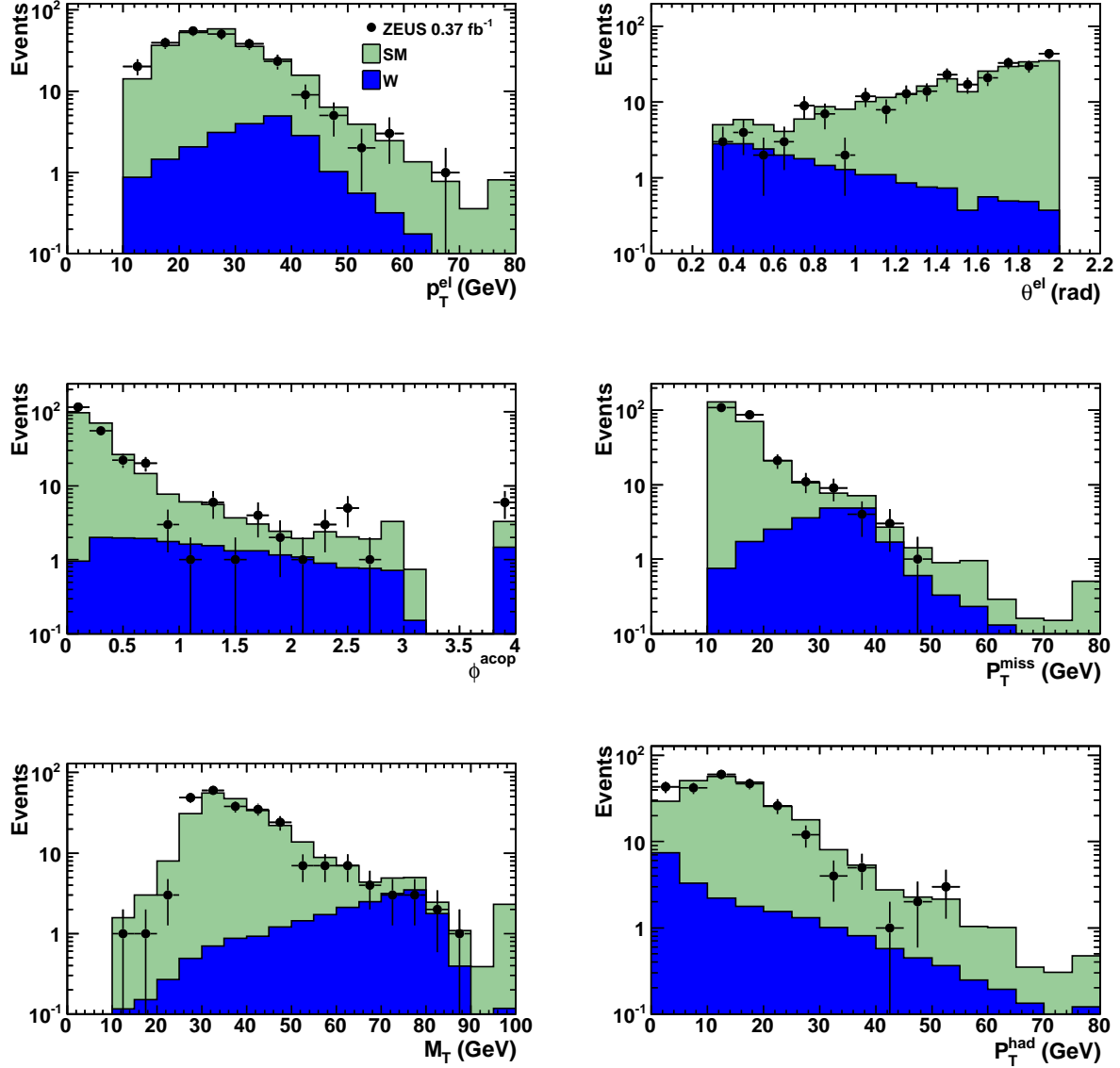


Figure 3: Comparison between data and SM expectations for several variables in the electron channel: p_T^{el} , θ^{el} , ϕ^{acop} , P_T^{miss} , M_T , P_T^{had} . The contribution of single-W production is also shown as the dark-shaded region. The last bin of the ϕ^{acop} histogram contains events with P_T^{had} less than 1 GeV for which ϕ^{acop} was not evaluated. In the other cases, any overflows are included in the last bin.

ZEUS

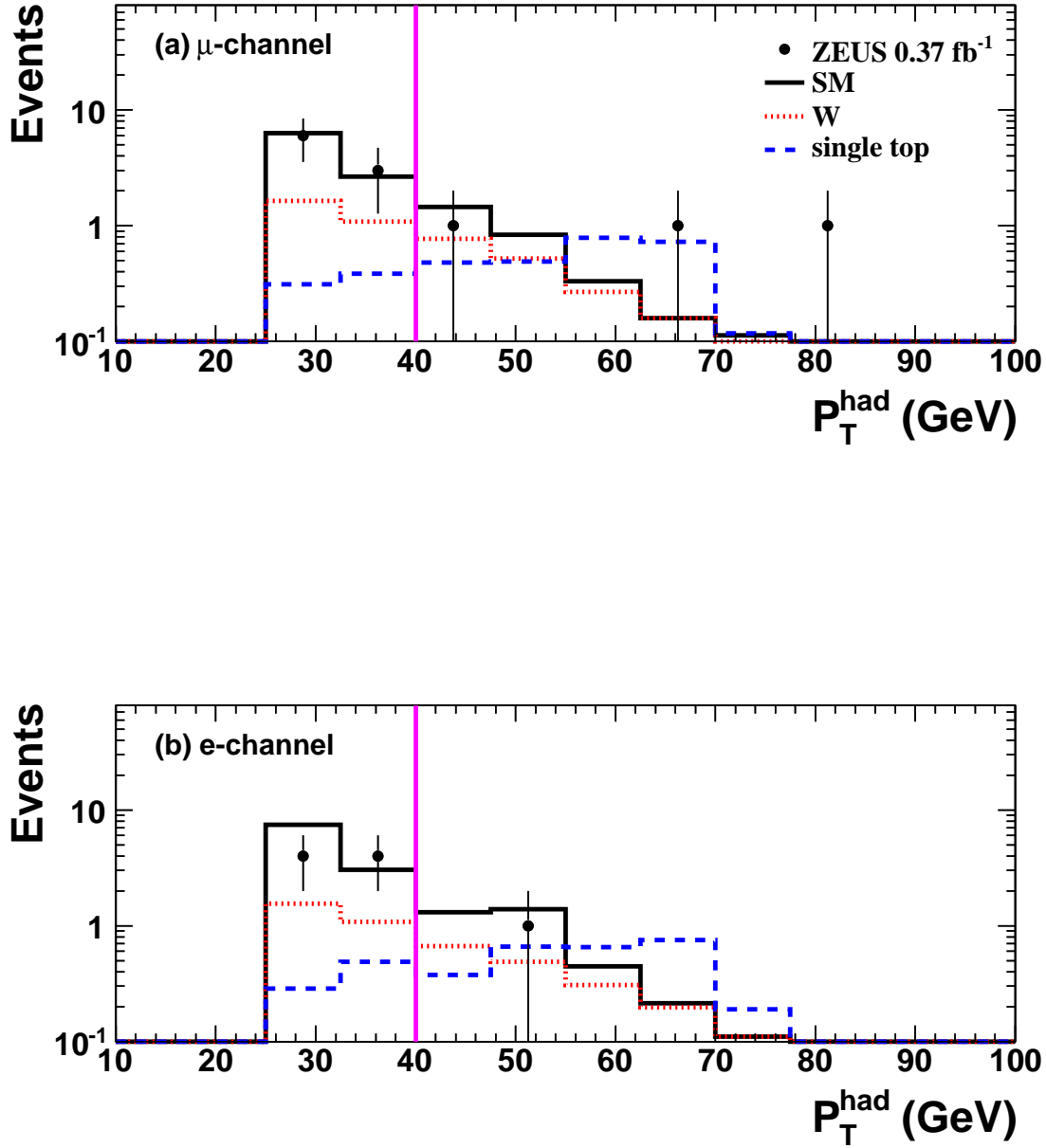


Figure 4: Comparison between data and MC expectations for the P_T^{had} distribution applying the final selection with a relaxed P_T^{had} cut at 25 GeV for (a) the muon and (b) the electron channel. The dots are the data, the solid histogram is the SM prediction including the W contribution, the dotted histogram the W contribution alone and the dashed histogram the single-top distribution normalized to the limit on the signal cross section of 0.24 pb (see Sect. 7.1). The final selection cut, $P_T^{\text{had}} > 40 \text{ GeV}$, is indicated.

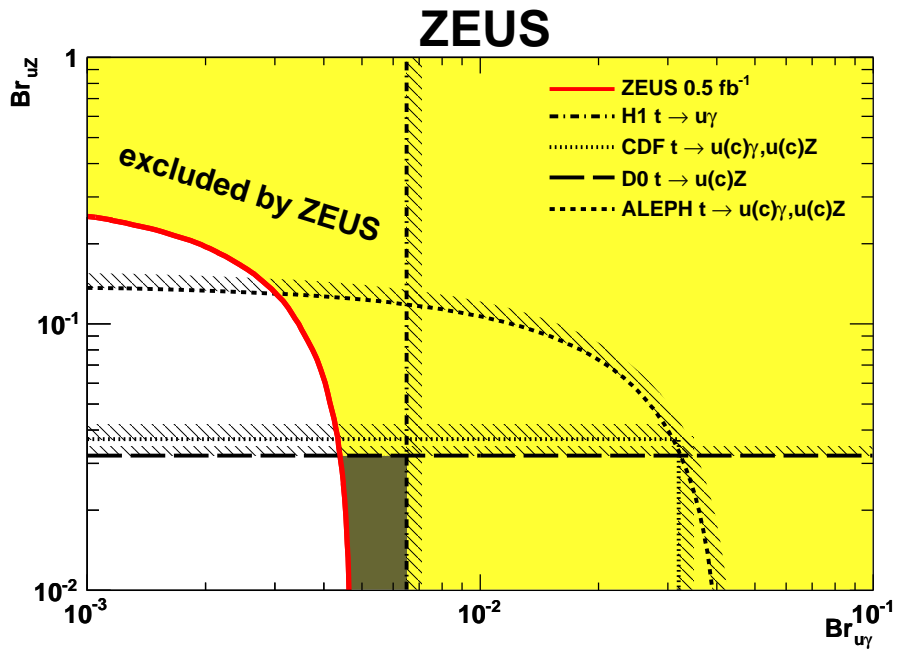


Figure 5: ZEUS boundary in the $(Br_{u\gamma}, Br_{uZ})$ plane. Also shown are boundaries of H1 [47], CDF [7], D0 [8] and ALEPH [10]. The shaded area is excluded. The dark shaded region denotes the area uniquely excluded by ZEUS.